nature cities

Article

https://doi.org/10.1038/s44284-026-00446-8

Tension between spatial pattern and hydrological adaptability in early Yangtze River Basin settlements

Received: 15 March 2025

Accepted: 23 April 2026

Published online: 22 May 2026

Check for updates

Jiayin Zhang (章佳茵)[1,2,3,10], Fang Wang (汪芳)[1,2,10] ✉, Ying Dong (董颖)[1,2,4,10], Shaoyi Mao (毛少羿)[1,2,4], Changping Zhang (张昌平)[5], Xie Hu (胡燮)[4], Chao Ning (宁超)[6], Jianli Chen (陈建立)[6], Jianbao Liu (刘建宝)[4], Yiyong Chen (陈义勇)[7], Jianguo Liu (刘建国)[8] & Qin Fang (方勤)[9]

Early settlements faced hydrological opportunities and constraints that informed transitions to urban living. Along the way, imbalances between urban expansion and infrastructural development and hydrological systems could threaten the sustainability of growing settlements. Here using archeological data and spatial modeling, we examine 2,106 early settlements dating from 8.5 ka BP to 2.72 ka BP in the middle reaches of the Yangtze River Basin. We trace how the distribution of settlements and hydrological conditions changed over time, focusing on associated trajectories of spatial pattern and hydrological adaptation. Results show that hydrological factors consistently influenced settlement patterns, even as settlements built infrastructure to manage floods and water access. Despite these efforts, cultural decline still occurred, revealing a persistent asymmetry between settlement pattern and hydrological adaptability. Our findings provide historical insight into how long-term vulnerabilities emerged in flood-prone environments, offering perspectives for understanding both past and future challenges in urban sustainability.

Interactions between urban systems and hydrological environments fundamentally play a central role in long-term social-ecological evolution, especially in flood-prone regions[1,2]. Contemporary expansion of communities in riverine areas has heightened urban vulnerability and risk exposure[3–5], and climate change and anthropogenic disturbances to water cycle are triggering increasingly complex hydrological challenges in these cities[6,7]. Critically, historical evidence indicates that hydrological constraints not only affect current conditions but are also profoundly ingrained throughout entire trajectories of urban rise and decline[8]. As proto-urban formations, early settlement patterns of hydrological engagement may contain deep-seated prototypes relevant to modern urban sustainability crises. And their adaptation strategies provide unique insights for understanding urban–water interactions[9,10].

Archeological records demonstrate how human societies have continually explored the boundaries of hydrological regulation through spatial interventions, from the very earliest small-scale technologies to the massive systems that sustained states. At the Pingliangtai site in the Huai River Basin, a roughly 5-hectare settlement

[1]Riv-Habitats Research Center, College of Architecture and Landscape Architecture, Peking University, Beijing, China. [2]Shanxi Key Laboratory of Watershed Built Environment with Locality (Peking University), Peking University, Beijing, China. [3]Department of Geography, University of California, Santa Barbara, CA, USA. [4]College of Urban and Environmental Sciences, Peking University, Beijing, China. [5]School of History, Wuhan University, Wuhan, China. [6]School of Archaeology and Museology, Peking University, Beijing, China. [7]School of Architecture and Urban Planning, Shenzhen University, Shenzhen, China. [8]Institute of Archaeology, Chinese Academy of Social Sciences, Beijing, China. [9]Hubei Provincial Institute of Cultural Relics and Archaeology Research, Wuhan, China. [10]These authors contributed equally: Jiayin Zhang, Fang Wang, Ying Dong. ✉e-mail: wfphd@pku.edu.cn

engineered a drainage system consisting of ceramic drain pipes, ditches and moats at about 4.1–3.9 ka BP[11]. In the lower Yangtze Delta, the ancient city of Liangzhu, with an estimated size of about 300 hectares, established a large-scale complex of dams, levees, ditches and other water-controlling features by 5.1 ka BP[12]. Further exemplifying this progression, the Khmer civilization in the Mekong Basin integrated water tanks, giant reservoirs, huge canals, rice fields and residential structures into the urban complex of Greater Angkor[13,14] by the 12th century AD within its circa 3,000-km^2 region[15], which is recognized to be the largest low-density preindustrial city on Earth. These transformative infrastructures may suggest a correlation between settlement spatial pattern and hydraulic sophistication. However, cross-regional comparisons across disparate developmental stages offer limited insights into the actual dynamics of hydrological adaptation.

How do changes in settlement spatial patterns compare with hydrological adaptability over time? This question demands investigation. Spatial pattern, which is manifested through settlement expansion, functional zoning and hierarchical organization, often facilitates complex hydraulic systems[12] but may simultaneously create systemic vulnerabilities. Unregulated expansion into floodplains, paired with infrastructure that is inadequate for climate variability, may increase exposure to hydrological stresses, leading settlements to become less stable and less viable over time. The collapse of Liangzhu culture (5.3–4.3 ka BP) in the lower reaches of the Yangtze River Basin exemplifies this disconnect. Along with numerous sites spreading over the Hangzhou–Jiaxing plain[16], the Liangzhu site was situated in a low-lying region characterized by strong variability in precipitation, where flooding normally occurs in June, followed by a dry and hot July–August. A terminal megadrought in4423±42 BP halted dam construction, and this infrastructural gap left the settlement defenseless against subsequent pluvial events[17], illustrating that spatial growth without adaptive capacity precipitates systemic failure.

Moreover, complex structural systems may operate effectively during relatively stable climates but reach tipping points under abrupt hydrological stresses[18]. Such historically conditioned configurations risk cascading failure during climatic perturbations, creating dissonance between form and function. The case of Angkor has been interpreted to exemplify this asymmetry, where its spatially sophisticated reservoir–canal network is claimed to have collapsed under monsoon extremes due to inflexible path dependencies[19]. This kind of vulnerability has been posited to have been echoed in Medieval Sri Lanka and Maya civilizations[20–22]. Collectively, these cases have been taken to indicate that spatial expansion and organizational improvement do not inherently confer regulatory capacity, particularly when infrastructure locks societies into rigid adaptation pathways under changing social and environmental circumstances.

We therefore focus on the middle reaches of China's Yangtze River Basin (8.5–2.72 ka BP), a region characterized by flat terrain, numerous rivers and lakes and long-term shaping by the East Asian monsoon, with wet summers and dry winters creating seasonal cycles of floods and droughts (see Methods for more details). As the early stage, when ancestors in the Yangtze River Basin explored their ecological environment and managed the human–environment relationship, this area provides an ideal context for exploring the intertwined temporal trajectories of spatial patterns and hydrological adaptability. Here we adopt a multiscalar spatial analytical perspective to examine trajectories of spatial change by analyzing settlement distribution patterns across regional, settlement-cluster and individual-site scales, as different scales may capture different social or environmental processes[23]. Hydrological adaptability refers to the capacity to respond to both hydrological opportunities and constraints through strategies such as flood control systems, irrigation networks and environmentally suitable site selection. Specifically, we investigate how early settlements adapted to hydrological dynamics and how such adaptation interacted with the emerging forms of spatial patterns. Drawing on a database of 2,106 settlements, this study reconstructs the long-term dynamics of spatial pattern and hydrological adaptation across six periods (Table 1), revealing tension between them and their implications for settlement sustainability. By integrating archeological reports, environmental proxies and spatial modeling, we advance the understanding of urban dynamics in flood-prone landscapes while demonstrating the capacity of long-time-series research to inform broader interdisciplinary dialogues on sustainability, resilience and urban adaptation.

Table 1 | Chronological framework and cultural sequences discussed in this study

Period	Time range (ka BP)	Cultures (ka BP)
Early Neolithic	8.5–6.3	Pengtoushan (8.5–7.8) Zaoshixiaceng (7.8–6.9) Tangjiagang (6.9–6.3) Chengbeixi (7.8–6.3) Bianfan (6.9–5.9)
Middle Neolithic	6.3–5.3	Daxi (6.3–5.5) Youziling (5.9–5.3)
Late Neolithic–Qujialing culture	5.3–4.5	Qujialing (5.3–4.5)
Late Neolithic–Shijiahe culture	4.5–3.9	Shijiahe (4.5–3.9)
Shang period	3.55–2.996	/
Western Zhou period	2.996–2.72	/

Results

Spatial patterns and hydraulic facilities

Early settlement patterns in the middle reaches of the Yangtze River Basin are observed at multiple spatial scales. Site numbers peaked in the Shang period, and total area peaked in the Shijiahe culture. At the regional scale, during the Neolithic Age, according to settlement sizes (Extended Data Table 1), large settlements accounted for the highest proportion among all settlements, yet the number of extra-large settlements was constantly on the rise. Nineteen of these settlements evolved into walled towns, which are defined as settlements enclosed by walls and moats, such as the Shijiahe walled town, Chenghe walled town and Yinxiang walled town[24]. By the Shang and Western Zhou periods, an increasing number of small and medium-small-sized settlements emerged around large and extra-large settlements. Extended Data Fig. 1 illustrates the distribution of settlement sizes.

The changes in settlement sizes at the regional level are also reflected in the spatial clustering of different settlements. We identified spatially clustered settlements from different periods. As shown in Extended Data Fig. 2, in the Early Neolithic period (8.5–6.3 ka BP), such clusters were mainly composed of large, medium-sized and medium-small-sized settlements. During the Middle Neolithic period (6.3–5.3 ka BP), walled towns began to develop within settlement clusters, surrounded by large and medium-sized settlements, with size disparities between settlements within the cluster becoming increasingly pronounced. By the Qujialing cultural period (5.3–4.5 ka BP), some settlement clusters, such as cluster 02, began to include multiple walled towns. In the Shijiahe cultural period (4.5–3.9 ka BP), the number of settlement clusters increased substantially. Settlement cluster 01, with the Shijiahe walled town as its center (Extended Data Fig. 3), gradually expanded into an aggregated settlement cluster with a center and functional zones[25]. The trend of a multipolar pattern within settlement clusters continued into the Western Zhou period (Extended Data Figs. 4 and 5).

At the individual-site scale, the spatial patterns more directly reflect interactions with the environment, as evidenced by corresponding hydraulic infrastructure. Early humans introduced water from outside the settlements into the interior through diversion trenches and

https://doi.org/10.1038/s44284-026-00446-8

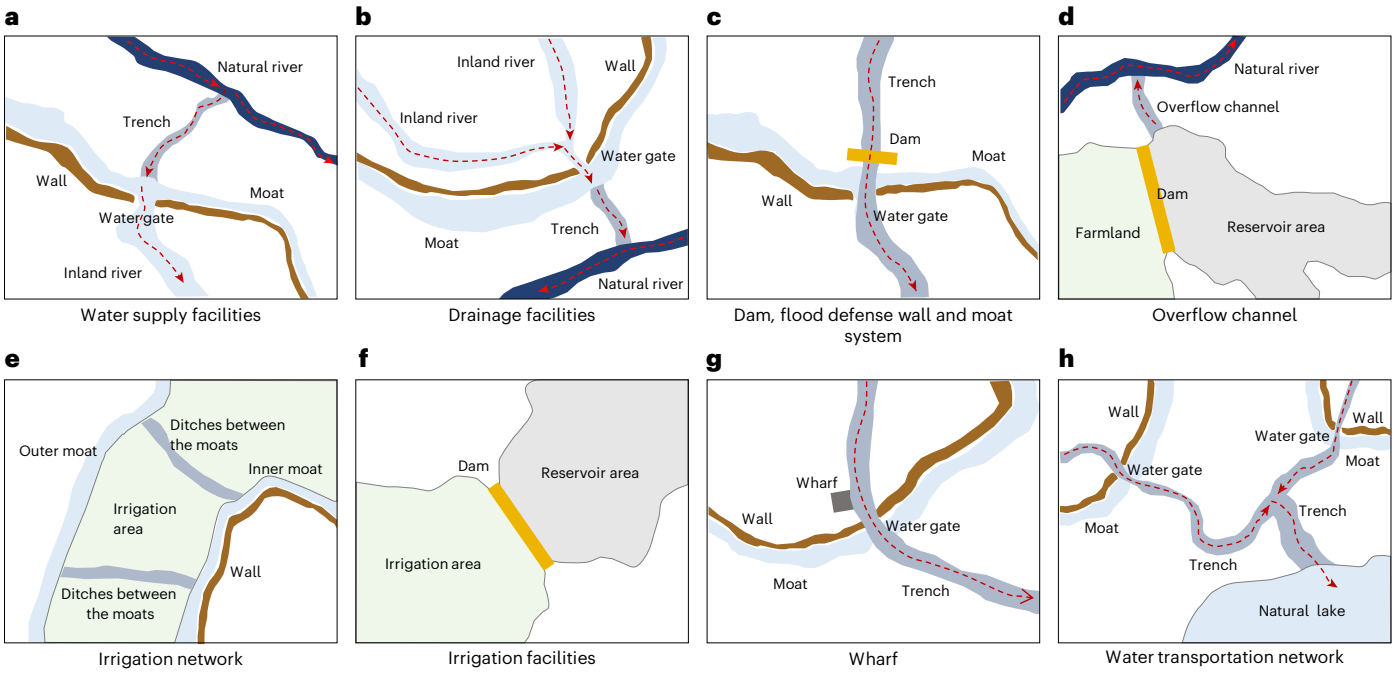

Fig. 1 | Hydraulic facilities of early settlements in the middle reaches of the Yangtze River Basin. a,**b**, Water supply (**a**) and drainage (**b**) facilities. **c**,**d**, Flood control structures: dam, food defense wall and moat (**c**) and an overflow channel (**d**). **e**,**f**, Irrigation systems: an irrigation network (**e**) and a reservoir-dam-irrigation system (**f**). **g**,**h**, Water transportation infrastructure: a wharf (**g**) and a water transportation network (**h**). Red dashed arrows indicate water flow direction.

water gates to form inland rivers (Fig. 1a) and then drained out via water gates and drainage trenches at lower elevations (Fig. 1b). Archeological findings (Supplementary Table 1) show the presence of water gates in some settlements. During the Shang and Western Zhou periods, water management infrastructure advanced further, as evidenced by the discovery of wells used for water extraction[26].

As the spatial structure of early settlements evolved across multiple scales, these communities evolved diverse hydrological adaptation strategies such as flood control, irrigation and water storage to regulate water resources. To defend against floods, early settlements mobilized manpower and resources to construct walls and moats. Many of these features are found in the Qujialing and Shijiahe cultural periods (5.3–3.9 ka BP) (Supplementary Table 2). The stratigraphic evidence from many moat excavations suggests that water flow rates were managed and stabilized, thereby reducing the risk of flooding within settlements[27]. The highest points of the walls were higher than or close to the warning flood level, thus acting as barriers against floodwaters[28], and dams outside the walls prevented rapid water flow from damaging the walls and provided additional flood protection[25] (Fig. 1c).

Among them, the Qixingdun walled town was equipped with a dual wall structure[29]. Zoumaling walled town exhibits an even more sophisticated wall system. Its walls were divided into inner and outer ones, both presumably surrounded by moats. An additional arc-shaped wall has been identified on the north side of the outer town, forming a defensive structure similar to that of a 'barbican', also accompanied by a relatively intact outer moat[24]. Similar to the function of moats, overflow channels were mostly used as flood control channels for water conservancy facilities such as reservoirs (Fig. 1d). Such water channels for flood release have been found in walled towns such as Shijiahe, Chenghe and Taojiahu[25,28].

In terms of drought resistance and irrigation, the Jijiaocheng settlement featured ditches between moats as well as inner and outer moats enclosing paddy fields to create controlled irrigation zones[30] (Fig. 1e). Another common pattern combined water storage areas, dams and irrigated fields, as confirmed by the Xiongjialing and Zhengfan dams at the Qujialing settlement[31] (Fig. 1f). These systems relied on seasonal storage and controlled release, where dams retained rainwater and ditches facilitated its redistribution for agricultural use.

Early settlements also carried out cultural and material exchanges through water transportation facilities. For example, there were similar wharf facilities at the Chengtoushan and Qixingdun walled towns[29,32] (Fig. 1g), and some moats might have served navigational purposes[27], connecting settlements to natural rivers and lakes through artificially dug trenches (Fig. 1h). In sites like Panlongcheng[33] during the Shang period and Miaotaizi[34] during the Western Zhou period, waterway transportation between the moats and outer rivers allowed for north–south material and cultural exchanges, likely contributing to their development as urban hubs and political centers.

Settlement distribution and hydrological dynamics

Despite the diverse adaptive modifications early settlements made to water, these practices predominantly focused on smaller and more manageable waterways. From the Early Neolithic period to the Western Zhou period, small rivers remained the primary choice for settlement locations (Extended Data Table 2). Taking the Dongting Lake Plain within the study area as an example, Fig. 2 visualizes settlement distribution patterns together with lake levels, hydrological conditions, major climatic events, flood probability density and hydrological adaptation. The following analysis draws on this figure.

The abrupt 8.2 ka BP climate event caused East Asia to experience a process of cooling and drying, followed by a rapid return to warm and humid conditions[35]. During the Pengtoushan to Zaoshixiaceng cultural period, lake levels steadily rose[36]. Although the rate of lake-level rise began to slow around 7.0 ka BP (ref. 37), settlement numbers remained low under these relatively high lake levels and were primarily located at higher elevations. From 5.5 ka BP to 4.0 ka BP, the abrupt cold and dry climate event around 5.5 ka BP led to reduced precipitation and lower lake levels[38]. However, as indicated by the flood probability density curve, the number of settlements in this area increased slowly during the Qujialing cultural period, a time with more temporally

https://doi.org/10.1038/s44284-026-00446-8

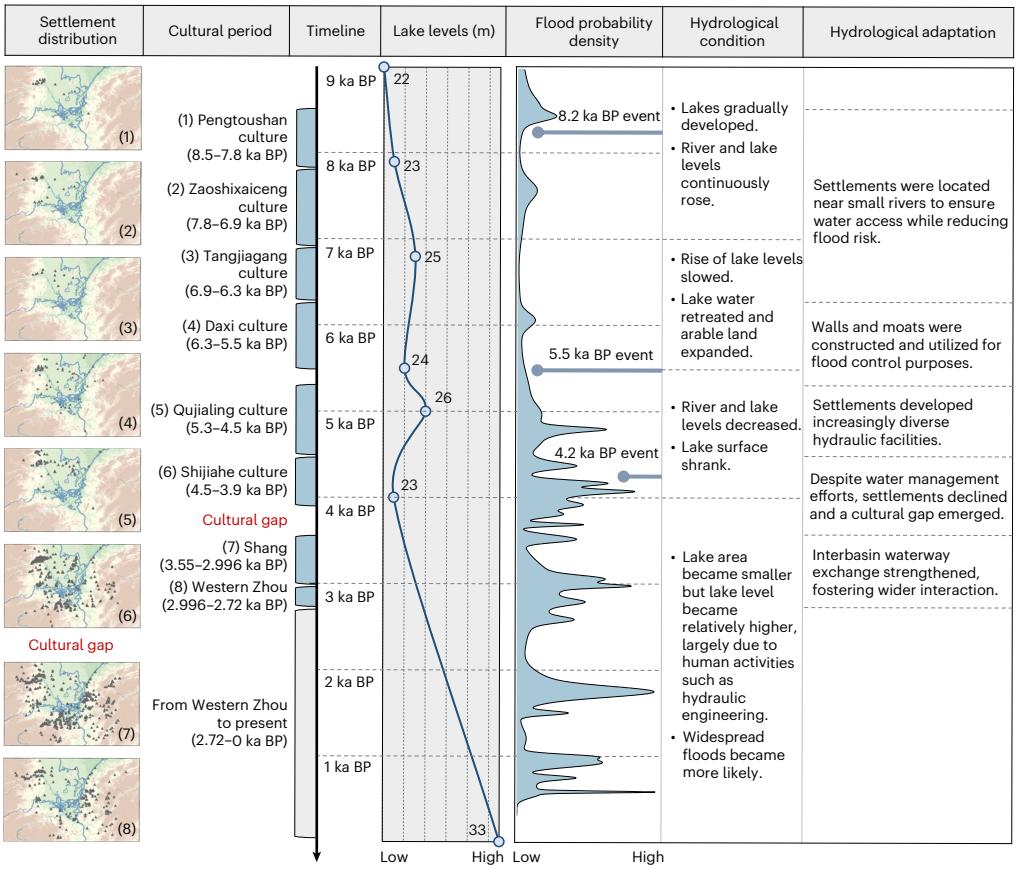

Fig. 2 | Distribution of early settlements in the Dongting Lake Plain alongside hydrological, climatic and adaptive contexts. Settlement distribution maps are not aligned to the time axis; each map corresponds to the labels in the 'Cultural period' column. Lake levels and flood probability density were obtained from previous research and adapted with permission from ref. 36, Sage; ref. 53, Elsevier. Elevation basemap derived from DEM based on Shuttle Radar Topography Mission (SRTM) v.4.1, NASA/CGIAR-CSI, available at https://srtm.csi.cgiar.org/srtmdata/.

concentrated flood-related evidence. By the Shijiahe cultural period, when lake levels reached their lowest point, the number of settlements increased substantially, marking a period of cultural prosperity in the Neolithic era.

The 4.2 ka BP climate event brought cooler and drier conditions to the middle reaches of the Yangtze River Basin[39], followed by a period in which the flood probability density curve shows a higher concentration of dated flood-related evidence from ~4.2 ka BP to 3.6 ka BP. During this period of catastrophic climate[17], primitive rice farming became difficult to sustain. At the same time, lakes expanded and lake levels rose, and many prehistoric settlements no longer maintained viable living conditions. These changes coincided with the decline of Neolithic culture and a widely recognized cultural gap, referring to a period marked by reduced settlement activity and discontinuity in cultural development[37]. By the Shang period, both the mainstream and tributaries of the Yangtze River had undergone substantial downcutting, reducing flat areas' susceptibility to flooding. This provided suitable spaces for human habitation along the Yangtze River, providing critical environmental conditions for the rise of settlements distributed along the river[40]. As illustrated in Fig. 2, by the Western Zhou period (around 3.0 ka BP), the flood probability density curve exhibits a pronounced signal, alongside high lake levels, coinciding with a reduction in the number of settlements. The lake level rose to 33 m in the modern period, when the lake area became smaller but the water level became higher than in the mid-Holocene, largely due to human activities such as hydraulic engineering[36].

Although exact temporal alignment between hydrological events and settlement changes remains challenging due to resolution differences in archeological and paleoenvironmental data, the cultural gap between the Shijiahe culture and the Shang period nonetheless suggests that early settlements may have been vulnerable to flood impacts.

Environmental factors of settlement distribution

This section analyzes the relationship between settlement distribution and four categories of environmental factors (for specific variables and their abbreviations, see Supplementary Table 3) based on the maximum entropy model (MaxEnt). Supplementary Figs. 1–4 illustrate the distribution patterns of early settlements in relation to these factors. In the Early Neolithic and Middle Neolithic, valley depth (VD) showed relatively high percent contributions (32.9% and 41.8%) and permutation importance (25.5% and 39%) (Extended Data Table 3), indicating that elevation relative to river valleys helped distinguish settlement locations from the background environment, as both metrics reflect the relative importance of predictor variables in the model. Presumably, VD is important because deeply incised valleys are more susceptible to flooding and often correspond to larger river systems. As shown in Fig. 3a, VD had the highest regularized training gain in these two periods, and the response curves (Fig. 3b) display a sharp increase in settlement probability above ~1,000 m in depth, suggesting a general preference for sites away from low-lying valleys.

In contrast, during the Late Neolithic (Qujialing culture and Shijiahe culture), VD's relative contribution declined (to 5.7% and 2.2%), and its permutation importance also dropped (5.5% and 0.6%). Other variables, such as distance to mega settlements and wind exposure, became more prominent (Fig. 3a and Extended Data Table 3). VD's response curve (Fig. 3b) shows increased settlement probability in

https://doi.org/10.1038/s44284-026-00446-8

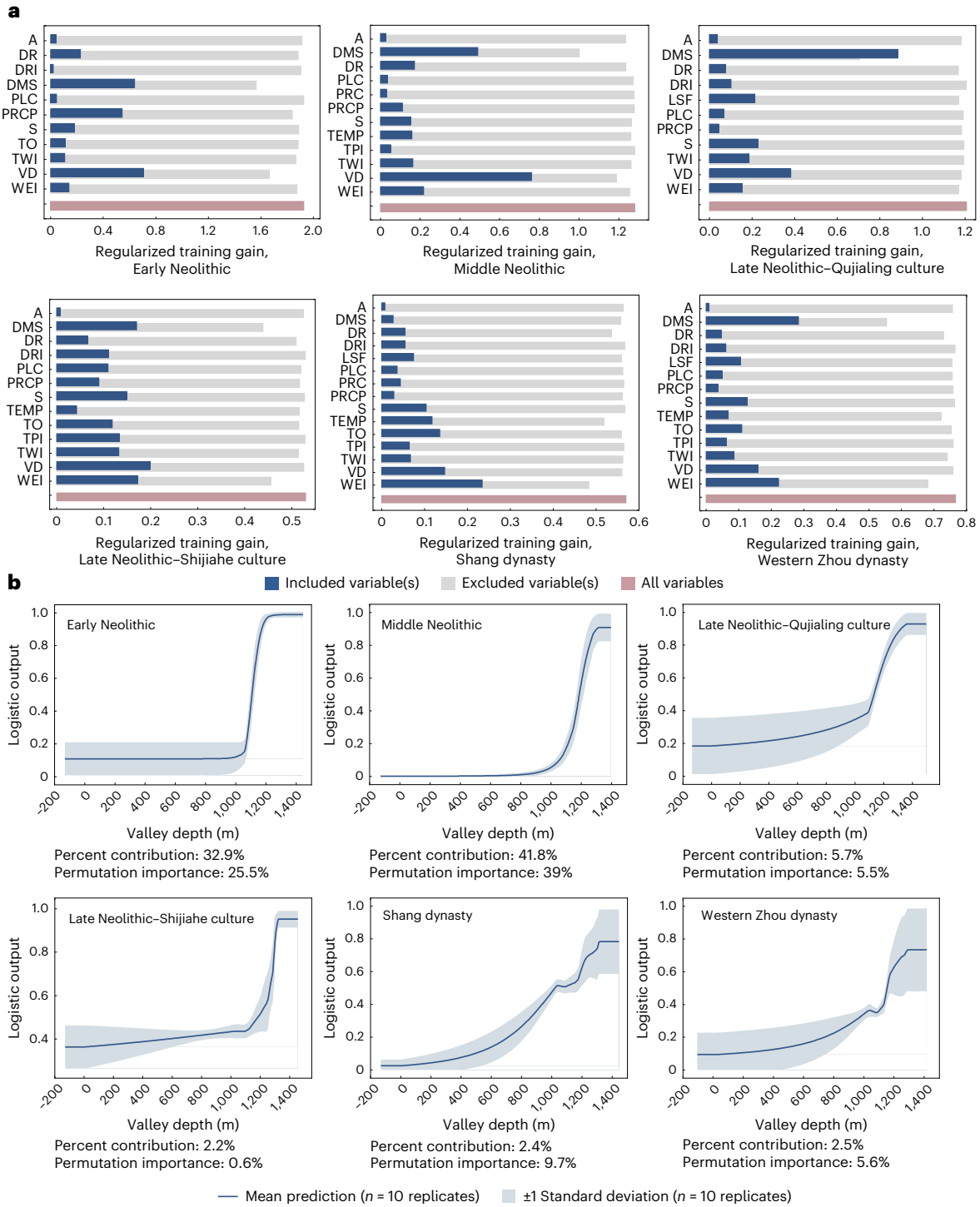

Fig. 3 | Environmental factors influencing the predicted distribution of early settlements across different periods based on the MaxEnt model. a, Results of the jackknife test of variable importance, based on regularized training gain. The bars reflect how much each variable contributes to the model's predictive ability when used alone and how much predictive power is lost when the variable is excluded. For each variable, the pink bar indicates the gain value when all variables are used to build the model; the dark blue bar represents the gain value when only the given variable is used to build the model, with higher gain values suggesting that the variable itself contains more critical information; and the gray bar shows the gain value when the specific variable is excluded and the model is built using the remaining variables. **b**, Response curves for VD across different periods. The curves show how the predicted probability of settlement occurrence (logistic output) varies with VD. The solid line represents the mean prediction across 10 replicate runs, and the shaded area indicates one standard deviation. The percent contribution and permutation importance of VD for each period are also reported. A, aspect; DR, distance to major river; DRI, direct insolation; DMS, distance to mega settlements; LSF, LS-factor; PLC, plan curvature; PRC, profile curvature; PRCP, precipitation; S, slope; TEMP, temperature; TO, topographic openness; TPI, topographic position index; TWI, topographic wetness index; VD, valley depth; WEI, wind exposure index.

lower valley areas than in earlier periods. A likely explanation is the decline in river levels earlier discussed, which reduced vertical distance and increased the habitability of valley bottoms. In the Shang and Western Zhou periods, VD maintained relatively minor importance across all indicators.

These results suggest that VD had greater influence in earlier periods and less in later ones, possibly reflecting the development of hydrological adaptation. However, the development of hydrological adaptation during this time did not prevent the emergence of a cultural gap between the Shijiahe and Shang periods. The collapse or weakening of regional settlement systems suggests that improvements in environmental adaptation were not sufficient to offset broader social, political, or ecological vulnerabilities.

Discussion

Archeological evidence from 8.5 ka BP to 2.72 ka BP in the middle reaches of the Yangtze River Basin captures the emergence of deliberate settlement planning and proto-urban spatial differentiation, although these early settlements differed from modern towns in concept, scale and structure. During the Early Neolithic period (8.5–6.3 ka BP), the Bashidang site saw the prototype of walled settlements, with artificial earthen walls found along the edges of the moat[41]. This indicates a shift from small individual settlements to more organized communities requiring coordinated labor and planning. By the Middle Neolithic (6.3–5.3 ka BP), the Chengtoushan site featured walls and moats enclosing the settlement, alongside signs of early urbanization such as the use of baked bricks for construction, increased presence of waste-related insect species and evidence of environmental degradation, making it one of the earliest known urbanized sites in China[32]. The Qujialing cultural period (5.3–4.5 ka BP) witnessed the emergence of hierarchical walled towns[42], including large and medium-sized sites such as Taojiahu, Chenghe and Majiayuan, as well as smaller walled towns.

During the Shijiahe cultural period (4.5–3.9 ka BP), the Shijiahe walled town emerged as a regional center, covering an area of 1.2 million m^2, with more than 40 surrounding settlements and possibly trade relations with neighboring settlements[25], forming a large-scale settlement cluster. By the Shang period (3.55–2.996 ka BP), the emergence of dynastic rule in the middle reaches of the Yangtze River Basin is exemplified by the Panlongcheng, which included palace remains and functioned as a regional node closely integrated into the early Shang political network centered around the capital in the Yellow River Basin[33]. During the Western Zhou period (2.996–2.72 ka BP), the capital system evolved into a multicentered structure, and the regime governed an extensive network of cities and settlements stretching from the Yellow River heartland into the middle reaches of the Yangtze River Basin[43]. By this time, the scale and intensity of human activity differed greatly from the Early Neolithic.

However, an asymmetry existed between the trajectories of spatial pattern and hydrological adaptation in early settlements between 8.5 ka BP and 2.72 ka BP. Settlements were typically located near small rivers and in low-elevation areas, where water sources were convenient and flood risks were lower. They also constructed hydraulic infrastructure like dams, reservoirs and irrigation canals to balance the demands for water access and flood/drought control. Even where settlement spatial patterns suggest efforts to address hydrological challenges, episodes of extreme flooding still disrupted long-term settlement continuity.

After the period examined in this study, hydrological adaptation among settlements in the middle reaches of the Yangtze River Basin also advanced continuously. From the Spring and Autumn period onward, the use of irrigation canals and storage ponds became more widespread[44]. By the Qin Dynasty, hydraulic projects on a huge scale were constructed, including the Ling Canal, which connected a major tributary of the middle Yangtze River with the Pearl River system[45]. Advancements in flood control technologies enhanced the capacity of settlements to regulate and utilize water resources, enabling an increasing number of large cities to stabilize and flourish along the Yangtze River. However, the gradual extension of settlement distribution into lower-lying areas also increased those settlements' susceptibility to flood inundation to some extent. Cities like Wuhan, situated at river confluences, benefited from these improved conditions and experienced sustained growth. However, despite advancements in water management, extreme flood events such as the 1998 Yangtze River flood continued to cause severe damage to settlements[46], showing the long-standing challenges of coexisting with dynamic hydrological systems.

In sum, as settlement spatial patterns evolved over time, settlement systems remained vulnerable to hydrological fluctuations, particularly under extreme conditions. The origin of human settlements is closely tied to rivers, yet achieving sustainable coexistence with water has remained a persistent challenge. Future research may seek to quantify the uneven or non-synchronous relationships between settlement spatial patterns and hydrological dynamics suggested by this study.

Methods

Case studies

The middle reaches of the Yangtze River Basin represent a key region where Chinese civilization originated, spread and integrated. As early as the Neolithic period, this area had established distinct cultural regional patterns, fostering an early riverine civilization rooted in agriculture. The favorable topography and abundant water resources here supported numerous early settlements, reflecting a symbiotic relationship between humans and water. Early inhabitants relied on water resources for agriculture, fishing and industrial production while also contending with hydrological risks such as flooding and drought.

This study focuses on the Jianghan–Dongting Basin, encompassing the Jianghan and Dongting plains in the middle reaches of the Yangtze River Basin. This basin was not only a major hub for production and daily life but also one of the six primary cultural regions of Neolithic archeology in China. It is characterized by a distinct cultural framework, with settlements and cultures evolving in a unified and synchronized manner, making it an ideal case for examining the environmental adaptations of early settlements. The geographical boundaries of the Jianghan–Dongting Basin remain undefined in a standardized sense. For this study, the region is delineated as including the plains within the basin and adjacent foothill zones aligned with specific administrative divisions. The spatial scope, locational outline and settlement distribution of the study area are depicted in Supplementary Fig. 5.

The relationship between humans and water in river basin settlements has undergone a lengthy evolution, and understanding the hydrological adaptability of early settlements is essential for uncovering long-term historical patterns. This study focuses on the broadly defined pre-Qin period, excluding the Paleolithic era, when few settlement remains are found, and the Eastern Zhou period, marked by social upheaval. This period represents an early phase in which humans explored their ecological environments and sought to harmonize human–environment interactions. Based on relevant literature on the chronological division of the Neolithic period[37,47] and the distribution of settlement numbers, it can be roughly divided into six temporal segments (Supplementary Fig. 6):

Early Neolithic (8.5–6.3 ka BP): The initial stage of human settlement development, characterized by small and individual settlements. In the Early Neolithic period, the earliest Neolithic culture in the Yangtze River Basin, the Pengtoushan culture (8.5–7.8 ka BP), was discovered in the Lishui region. Subsequently, two cultural stages, the Zaoshixiaceng culture (7.8–6.9 ka BP) and the Tangjiagang culture (6.9–6.3 ka BP), developed. In the Xiajiang region of western Hubei province, the Chengbeixi culture (7.8–6.3 ka BP), originating from the Pengtoushan culture, emerged. Meanwhile, in the central area of the eastern Han River in the Jianghan Plain, the Bianfan culture (6.9–5.9 ka BP) appeared.

Middle Neolithic (6.3–5.3 ka BP): The first walled town in China, Chengtoushan, developed in the middle reaches of the Yangtze River Basin. In the Middle Neolithic period, following the Chengbeixi and Tangjiagang cultures, the Xiajiang region and Lishui region developed the Daxi culture (6.3–5.5 ka BP). The Jianghan Plain relatively independently developed the Youziling culture (5.9–5.3 ka BP).

Late Neolithic–Qujialing culture (5.3–4.5 ka BP): The Qujialing culture emerged, unifying the civilization of the middle reaches of the Yangtze River Basin, with an increase in the scale and number of settlements and walled towns.

Late Neolithic–Shijiahe culture (4.5–3.9 ka BP): The Shijiahe culture represented an important stage of Neolithic complexity in the middle reaches of the Yangtze River Basin, with the Shijiahe walled town serving as a central hub within this regional network.

Shang period (3.55–2.996 ka BP): Around 3.9 ka BP, Neolithic culture in the middle reaches of the Yangtze River Basin declined, but settlement activity continued during the Shang period. The Shang court, centered in the Yellow River Basin, established a southern outpost at Panlongcheng site, introducing Central Plains spatial patterns into the region.

Western Zhou period (2.996–2.72 ka BP): In the Western Zhou period, the royal court established a hierarchical network of settlements in the middle Yangtze River basin through the system of enfeoffment, further shaping regional spatial structures. Meanwhile, diverse cultural elements from surrounding river basins entered the region along major waterways.

Data collection

To investigate the relationship between spatial patterns and hydrological adaptation in early settlements, it is necessary to combine archeological and environmental data. In terms of settlement data, this study vectorized the settlement site information recorded in *The Atlas of Chinese Cultural Relics: Hubei Volume*[48] and *The Atlas of Chinese Cultural Relics: Hunan Volume*[49], supplementing it with recent archeological excavation reports from the relevant regions. The settlement information in the *Atlas* comes from the second national cultural relics survey, which comprehensively documented the condition of all known immovable cultural heritage sites across China. Notably, as the data are primarily derived from sporadic rescue excavations rather than systematic surveys, they do not represent a comprehensive and accurate reflection of the distribution of ancient settlements and lack key information such as population and social structure[50]. These limitations are particularly likely to affect the Neolithic period, for instance, leading to the underestimation of the number and scale of settlement sites. Although there are limitations to modeling early settlements using *The Atlas of Chinese Cultural Relics*, this study has attempted to complement the *Atlas* data with other archeological excavation reports to reconstruct the scale, structure and hydraulic facilities of settlement sites across different periods. Overall, the data still provide an opportunity to observe the macro-level spatial patterns of early settlements in the Jianghan–Dongting Basin. After image correction and map registration, the settlement points were vectorized, and a corresponding spatial database was established using ArcGIS Pro 3.3. The spatial database includes attributes such as longitude and latitude, city/county, township, settlement name, period and area. The study covers a total of 2,106 settlement sites in the Jianghan–Dongting Basin, including 61 Early Neolithic settlements, 125 Middle Neolithic settlements, 192 Late Neolithic–Qujialing culture settlements, 678 Late Neolithic–Shijiahe culture settlements, 684 Shang settlements and 395 Western Zhou settlements. Due to temporal overlaps among some sites, the total number is slightly lower than the sum of each period.

River data were derived from topographic data. Due to the lack of paleotopographic reconstruction data, this study uses modern digital elevation models (DEMs) to analyze the macro spatial distribution of settlements. Since the end of the Last Glacial Maximum, tectonic activity in the middle reaches of the Yangtze River Basin has slowed, and the macro topographic features are relatively close to modern ones, making the use of modern DEM data to extract relevant topographic information feasible. The DEM data used in this study come from the Shuttle Radar Topography Mission (SRTM) conducted by NASA's Space Shuttle *Endeavour*. The data are based on the latest SRTM V4.1, resampled and projected using the WGS-84 ellipsoid with a spatial resolution of 250 m. Based on these topographic data, hydrological analysis was conducted using the Hydrology tools in the Spatial Analyst toolbox of ArcGIS Pro 3.3 to extract and classify river systems, with default parameters applied. The extracted rivers were categorized into six hierarchical levels according to their upstream flow accumulation and network position.

Precipitation and temperature data come from the CAS-FGOALS dataset, which reconstructs the multiyear average of precipitation and temperature conditions during the mid-Holocene (6 ka BP)[51]. Although meteorological and climatic conditions varied across different periods, the relative regional differences remained largely consistent[52]. The flood probability density curve for the middle Yangtze River is extracted from relevant literature[53], and the historical lake-level curve is also based on reconstructed Dongting Lake levels from a relevant study[36].

According to the literature mentioned above, the generation of the flood probability density curve for the middle Yangtze River primarily adopted the cumulative probability distribution method commonly used in archeology sites[54,55]. Specifically, it first screens 114 Holocene paleoflood records with robust evidence of flood occurrence (including clear timing and location of floods, and relying on objective geological entities rather than vague descriptions), then determines the age of each flood event through dating methods such as accelerator mass spectrometry radiocarbon and optically stimulated luminescence and finally treats each flood layer as an independent flood event. The chronological data of these flood events are input into the OxCal platform, and the Sum and C Data command is used to generate a probability density plot that reflects the relative frequency of floods. Although this curve does not capture information on flood frequency or intensity, it serves as a descriptive visualization of the relative concentration of dated flood evidence through time. Despite the inherent chronological uncertainty of radiocarbon dating and its calibration effects, it provides an approximate chronological framework for explaining the temporal dynamics of flood-related signals.

Based on the above-mentioned literature, the reconstruction of the historical lake levels of Dongting Lake was comprehensively accomplished by integrating archeological sites, geological data and climatic records. In detail, Neolithic sites on the lakeshore plain and floodplain were chosen, whereas those on artificially accumulated land or hills were excluded, to identify the minimum habitation elevation for each cultural stage. This base is defined as the 'minimum safe threshold for human habitation', and its elevation is derived by subtracting the total sediment thickness (encompassing cultural layers and soil) from the current surface elevation of each selected site. Furthermore, an assumption is made that the ancient lake level was 1–2 m lower than this base, which is based on the observed height difference between the modern Dongting Lake level and the habitable base. The validity of this reconstruction approach is mainly confirmed through the cross-verification of three types of evidence: the spatial distribution of Neolithic sites, the evolutionary patterns of the lake basin's morphology and climate fluctuations inferred from pollen analysis.

Although each dataset has limitations, such as uneven archeological survey intensity or reliance on modern elevation models, their combination provides a valuable opportunity to reconstruct the broader dynamics of settlement–environment interaction across long timescales. Rather than aiming for precise historical reconstruction, this study uses a comparative, regional approach to examine how spatial organization and environmental responses codeveloped in early settlement systems.

Extraction of settlement clusters

In the settlement cluster analysis, this study used the DBSCAN (density-based spatial clustering of applications with noise) clustering algorithm to extract settlement clusters. DBSCAN is a density-based spatial clustering algorithm that identifies all dense regions of sample points as clusters, making it suitable for clustering analysis of low-dimensional data. The algorithm requires two parameters to be adjusted: E_{ps} and Min_{pts}. E_{ps} refers to the neighborhood of a settlement within a given radius, and Min_{pts} is the minimum number of samples required within the E neighborhood. This study used the DBSCAN module in ArcGIS Pro 3.3 to perform settlement clustering. Based on the statistical characteristics of the dataset, we selected a search radius of 12 km and a minimum sample size of 5 for settlement cluster extraction and then validated the extracted clusters against actual pattern. A total of four settlement clusters were identified for the Early Neolithic period (one from the Pengtoushan culture, one from the Zaoshixiaceng culture, one from the Tangjiagang culture and one from the Chengbeixi culture), four for the Middle Neolithic period (one from the Youziling culture and three from the Daxi culture), five for the Late Neolithic–Qujialing culture, 20 for the Late Neolithic–Shijiahe culture, 17 for the Shang period and 15 for the Western Zhou period. During the Bianfan culture period, settlement sites were relatively dispersed and did not form distinct clusters.

Mechanism analysis of settlement spatial patterns

This study employed MaxEnt to analyze the mechanisms of settlement spatial patterns, implemented using MaxEnt 3.4.4 software (https://biodiversityinformatics.amnh.org/open_source/maxent/). MaxEnt is a machine learning method that is especially suitable for presence-only data, such as archeological settlement locations, because it does not require researchers to identify areas as definitely lacking settlements. Instead, it compares the environmental characteristics of known settlement points with a set of randomly sampled background points within the study area.

The model is based on the principle of maximum entropy, which assumes that the most appropriate prediction is the one that is most spread out or uniform, given the constraints provided by the known data. It uses the environmental features at the known settlement locations to estimate a probability distribution across space, choosing the distribution that best reflects the observed data while assuming the least additional information. Assuming the probability distribution of a discrete random variable x is $P(x)$, the entropy formula is as follows:

$$H(P) = -\sum_{x} P(x) \log P(x) \quad (1)$$

This is done under the condition that the expected values of environmental variables under $P(x)$ match the observed averages at the known settlement sites. The model then evaluates how much each environmental variable contributes to the distribution pattern. In this study, MaxEnt was used to compare the relative influence of environmental factors across six different periods. By evaluating how well each variable predicted the spatial distribution of settlements across different periods, we inferred the degree to which early settlements were responding to specific environmental conditions.

This study developed an indicator system that served as the environmental variable input for the MaxEnt model. The criterion layer included surface morphology, water adaptability, location attributes and meteorological and climatic conditions; specific indicators, calculation methods and abbreviations are provided in Supplementary Table 3. Except for distance to a major river, distance to mega settlements, precipitation and temperature, other variables were extracted from DEM data using the Saga GIS 7.9.0 automated geoscience analysis system. The Euclidean distances from each settlement to the nearest mega settlement and major river were calculated using the Euclidean Distance tool in ArcGIS Pro 3.3. All related variable data were resampled to a 250-m resolution and converted to ASCII format.

The selected variables exhibit certain correlations, such as the influence of slope on local terrain curvature. Excessive linear correlations between variables can complicate the interpretability of the model results. Therefore, variable screening was necessary before formally inputting the data into the model. First, Pearson correlation coefficients were calculated to test for collinearity between variables (Supplementary Fig. 7), retaining variables with correlations below 0.8. Correlation analysis and statistical visualization were performed using OriginLab 2022. Next, the selected variables and settlement distribution data were input into MaxEnt 3.4.4 to run an initial simulation model, generating the contribution rates of each variable to settlement distribution. For variable groups with correlations exceeding 0.8, the variable with the highest contribution rate was retained. Given that the contribution of variables varied across different periods, the final screened variables (Supplementary Table 4) included macroscale factors and local characteristics encompassing all four categories.

To account for the differing influence of settlements of varying sizes on spatial patterns, settlement points in the MaxEnt input files were weighted according to their area. Specifically, site areas were first standardized and then multiplied by 10 after rounding to one decimal place. The resulting value was used to duplicate each settlement point accordingly in the model input.

To account for potential sampling bias in archeological survey data, we constructed a bias layer[56] based on kernel density estimation of all known settlement locations across periods. The kernel density estimation was performed in ArcGIS Pro 3.3 using the Kernel Density tool. All 2,106 settlement points were used as input features. The output cell size was set to 250 m to match the resolution of the environmental layers. The search radius was set to 100,000 m, based on the exploratory sensitivity tests for optimal smoothing. The resulting raster bias layer highlighted zones with higher densities of known settlements and served as a proxy for differential survey effort, and it was provided to MaxEnt to guide background point sampling. By weighting background points according to this bias file, we mitigated the influence of uneven survey effort on model estimation.

This study randomly selected 75% of the total settlement points as training data and 25% as testing data, with a maximum iteration limit of 500. The model was run 10 times using the bootstrap method, where each replicate resamples the original data with replacement to assess the model's stability and variability. The results from the testing dataset were used to validate the accuracy of the training dataset. Model performance was evaluated using the area under the receiver operating characteristic curve (AUC). The AUC value ranges from 0 to 1, with values between 0.5 and 0.7 indicating low model accuracy, values between 0.7 and 0.9 indicating high accuracy and values above 0.9 representing the highest accuracy. After 10 repeated runs, the average AUC values for the six temporal phases were 0.972 (±0.010), 0.916 (±0.008), 0.909 (±0.014), 0.835 (±0.006), 0.839 (±0.005) and 0.857 (±0.010). The results remained stable across the 10 repeated runs, indicating that additional repetitions would not substantially improve model reliability.

To improve the robustness of interpretation, this study reports three indicators provided by MaxEnt to assess variable importance: percent contribution, permutation importance and jackknife test results. Percent contribution reflects the increase in the model's gain associated with each variable during the training process. Permutation importance measures the decrease in model performance (AUC) when the values of a variable are randomly permuted. A larger decrease indicates that the variable contains information not present in others. The jackknife test evaluates the independent and unique contribution of each variable. The model is run three times for each variable: using all variables, using only the variable of interest and excluding the variable. The resulting regularized training gain values help assess the

information content and substitutability of each variable: the greater the difference between the gain value when the specific variable is excluded and the model is built using the remaining variables, and the gain value when all variables are used to build the model, the more irreplaceable the information provided by the excluded variable.

Reporting summary

Further information on research design is available in the Nature Portfolio Reporting Summary linked to this article.

Data availability

The datasets used in this study, including the multiperiod settlement point distributions in the Jianghan–Dongting Basin, as well as all input files for the MaxEnt model (settlement points by period, environmental variable layers and the bias file), are available via Zenodo at https://doi.org/10.5281/zenodo.14517680 (ref. 57). Some data used in this study are from publicly available sources: the SRTM V4.1 DEMs can be accessed via the data search page at https://srtm.csi.cgiar.org/srtmdata/; the mid-Holocene CAS-FGOALS dataset is accessible at https://esgf-node.llnl.gov/search/cmip6/.

Code availability

No custom code was used in this study. The analysis was conducted using software mentioned in the Methods.

References

1. Devitt, L. et al. Flood hazard potential reveals global floodplain settlement patterns. *Nat. Commun.* **14**, 2801 (2023).
2. Rentschler, J. et al. Global evidence of rapid urban growth in flood zones since 1985. *Nature* **622**, 87–92 (2023).
3. Wannewitz, M. et al. Progress and gaps in climate change adaptation in coastal cities across the globe. *Nat. Cities* **1**, 610–619 (2024).
4. Tellman, B. et al. Satellite imaging reveals increased proportion of population exposed to floods. *Nature* **596**, 80–86 (2021).
5. Paprotny, D., Sebastian, A., Morales-Nápoles, O. & Jonkman, S. N. Trends in flood losses in Europe over the past 150 years. *Nat. Commun.* **9**, 1985 (2018).
6. Wang, H. et al. Anthropogenic climate change has influenced global river flow seasonality. *Science* **383**, 1009–1014 (2024).
7. Wu, J. et al. Global syndromes induced by changes in solutes of the world's large rivers. *Nat. Commun.* **12**, 5940 (2021).
8. Haug, G. H. et al. Climate and the collapse of Maya civilization. *Science* **299**, 1731–1735 (2003).
9. Smith, M. E. Why archaeology's relevance to global challenges has not been recognised. *Antiquity* **95**, 1061–1069 (2021).
10. Roberts, P. et al. Using urban pasts to speak to urban presents in the Anthropocene. *Nat. Cities* **1**, 30–41 (2024).
11. Li, C. et al. Earliest ceramic drainage system and the formation of hydro-sociality in monsoonal East Asia. *Nat. Water* **1**, 694–704 (2023).
12. Liu, B. et al. Earliest hydraulic enterprise in China, 5,100 years ago. *Proc. Natl Acad. Sci. USA* **114**, 13637–13642 (2017).
13. Evans, D. & Fletcher, R. The landscape of Angkor Wat redefined. *Antiquity* **89**, 1402–1419 (2015).
14. Fletcher, R. An opinion on issues for future investigation of the water management of Greater Angkor. *WIREs Water* **7**, e1474 (2020).
15. Klassen, S. et al. Diachronic modelling of the population within the medieval Greater Angkor Region settlement complex. *Sci. Adv.* **7**, eabf8441 (2021).
16. Zheng, H. et al. Spatial and temporal distribution of Neolithic sites in coastal China: sea level changes, geomorphic evolution and human adaption. *Sci. China Earth Sci.* **61**, 123–133 (2018).
17. Zhang, H. et al. Collapse of the Liangzhu and other Neolithic cultures in the lower Yangtze region in response to climate change. *Sci. Adv.* **7**, eabi9275 (2021).
18. Penny, D. et al. The demise of Angkor: systemic vulnerability of urban infrastructure to climatic variations. *Sci. Adv.* **4**, eaau4029 (2018).
19. Fletcher, R., Buckley, B. M., Pottier, C. & Wang, S.-Y. S. in *Megadrought and Collapse: From Early Agriculture to Angkor* (ed. Weiss, H.) Ch. 9 (Oxford Univ. Press, 2017).
20. Coningham, R. & Lucero, L. J. Urban infrastructure, climate change, disaster and risk: lessons from the past for the future. *J. Br. Acad.* **9**, 79–114 (2021).
21. Douglas, P. M. J. et al. Drought, agricultural adaptation, and sociopolitical collapse in the Maya Lowlands. *Proc. Natl Acad. Sci. USA* **112**, 5607–5612 (2015).
22. Medina-Elizalde, M. et al. High resolution stalagmite climate record from the Yucatán Peninsula spanning the Maya terminal classic period. *Earth Planet Sci. Lett.* **298**, 255–262 (2010).
23. Bevan, A. & Conolly, J. in *Confronting Scale in Archaeology: Issues of Theory and Practice* (eds Lock, G. & Molyneaux, B. L.) Ch. 14 (Springer, 2006).
24. Shan, S. et al. The emergence of walled towns in prehistoric middle Yangtze River valley: excavations at the Zoumaling site. *Archaeol. Res. Asia* **26**, 100285 (2021).
25. Fang, Q., Deng, Q. & Xiang, Q. *Shijiahe Discoveries and Studies* (Science, 2021).
26. Zhou, Y., Zwahlen, F. & Wang, Y. The ancient Chinese notes on hydrogeology. *Hydrogeol. J.* **19**, 1103–1114 (2011).
27. Mo, D. & Zhuang, Y. in *Water Societies and Technologies from the Past and Present* (eds Zhuang, Y. & Altaweel, M.) Ch. 4 (UCL, 2018).
28. Liu, J., Peng, X., Tao, Y. & Xiang, Q. *Prehistoric Water Management Civilization in the Jianghan Plain* (China Social Sciences, 2023).
29. Wang, L., Wu, R., Zhang, S. & Zhang, K. Brief report on the 2018 survey, coring and excavation of the Qixingdun site in Huarong County. *Archaeology* **02**, 3–19 (2021).
30. Fan, X. et al. Survey, coring, and trial excavations of the Jijiaocheng settlement cluster in Lixian County, Hunan. *Archaeology* **05**, 22–40 (2023).
31. Qujialing Site, Jingmen, Hubei. *National Cultural Heritage Administration* http://www.ncha.gov.cn/art/2024/3/27/art_2759_187899.html (2024).
32. Yasuda, Y. et al. Environmental archaeology at the Chengtoushan site, Hunan Province, China, and implications for environmental change and the rise and fall of the Yangtze River civilization. *Quat. Int.* **123–125**, 149–158 (2004).
33. School of History, Wuhan University, Hubei Provincial Institute of Cultural Relics and Archaeology, Wuhan Institute of Archaeology & Panlongcheng Site Museum. *Panlongcheng (1995–2019)* (ed. Zhang, C.) (Science, 2024).
34. Guo, C., Zhang, B., Zheng, W. & Zhang, C. Brief report on excavation of the Western Zhou remains at Miaotaizi in Suizhou, Hubei Province. *Jianghan Archaeol.* **01**, 3–14 (2022).
35. Zhao, W., Li, H., Chen, C. & Renssen, H. Large-scale vegetation response to the 8.2 ka BP cooling event in East Asia. *Palaeogeogr. Palaeoclimatol. Palaeoecol.* **608**, 111303 (2022).
36. Liu, T., Chen, Z., Sun, Q. & Finlayson, B. Migration of Neolithic settlements in the Dongting Lake area of the middle Yangtze River basin, China: lake-level and monsoon climate responses. *Holocene* **22**, 649–657 (2012).
37. Zhao, C. & Mo, D. Holocene hydro-environmental evolution and its impacts on human occupation in Jianghan-Dongting Basin, middle reaches of the Yangtze River, China. *J. Geogr. Sci.* **30**, 423–438 (2020).

38. Wu, W., Zheng, H., Hou, M. & Ge, Q. The 5.5 cal ka BP climate event, population growth, circumscription and the emergence of the earliest complex societies in China. *Sci. China Earth Sci.* **61**, 134–148 (2017).
39. Guo, A., Mao, L., Li, C. & Mo, D. Reconstruction of the paleoenvironmental context of Holocene human behavior at the Fenghuangzui site in the Nanyang Basin, Middle Yangtze River, China. *npj Herit. Sci.* **13**, 2 (2025).
40. Shelach-Lavi, G. *The Archaeology of Early China: From Prehistory to the Han Dynasty* (Cambridge Univ. Press, 2015).
41. Hunan Provincial Institute of Cultural Relics and Archaeology. *Pengtoushan and Bashitong* (Cultural Relics, 2006).
42. Zhang, C. in *A Companion to Chinese Archaeology* (ed. Underhill. A. P.) Ch. 25 (Blackwell, 2013).
43. Li, F. *Bureaucracy and the State in Early China: Governing the Western Zhou* (Cambridge Univ. Press, 2008).
44. Zhang, F. *History of Ancient Irrigation Engineering Technology in China* (Shanxi Education, 2009).
45. Yao, H. *History of Water Conservancy Development in China* (Shanghai People's, 2005).
46. Li, B., Yan, Q. & Zhang, L. Flood monitoring and analysis over the middle reaches of Yangtze River basin using MODIS time-series imagery. In *Proc. IEEE International Geoscience and Remote Sensing Symposium* 807–810 (IEEE, 2011).
47. Deng, H., Chen, Y., Jia, J., Mo, D. & Zhou, K. Distribution patterns of the ancient cultural sites in the middle reaches of the Yangtze River since 8500 a BP. *Acta Geogr. Sin.* **64**, 1113–1125 (2009).
48. National Cultural Heritage Administration. *The Atlas of Chinese Cultural Relics: Hubei Volume* (Xi'an Cartographic, 2002).
49. National Cultural Heritage Administration. *The Atlas of Chinese Cultural Relics: Hunan Volume* (Hunan Cartographic, 1997).
50. Jaffe, Y. Y., Castellano, L., Shelach-Lavi, G. & Campbell, R. B. Mismatches of scale in the application of paleoclimatic research to Chinese archaeology. *Quat. Res.* **99**, 14–33 (2020).
51. Zheng, W. et al. CAS-FGOALS Datasets for the two interglacial epochs of the Holocene and the Last Interglacial in PMIP4. *Adv. Atmos. Sci.* **37**, 1034–1044 (2020).
52. Demján, P. et al. Long time-series ecological niche modelling using archaeological settlement data: tracing the origins of present-day landscape. *Appl. Geogr.* **141**, 102669 (2022).
53. Zhang, Z. et al. A review of paleofloods in the middle-lower reaches of the Yangtze River during the Holocene: processes, causes and effects. *Quat. Sci. Rev.* **345**, 109019 (2024).
54. Dong, G. et al. Evolution of human–environmental interactions in China from the Late Paleolithic to the Bronze Age. *Prog. Phys. Geogr.* **44**, 233–250 (2019).
55. Zhang, J. et al. Crossing of the Hu line by Neolithic population in response to seesaw precipitation changes in China. *Sci. Bull.* **67**, 844–852 (2022).
56. Kramer-Schadt, S. et al. The importance of correcting for sampling bias in MaxEnt species distribution models. *Divers. Distrib.* **19**, 1366–1379 (2013).
57. Zhang, J. et al. Early settlement and environmental dataset for the Jianghan-Dongting Basin (8.5–2.7 ka BP). *Zenodo* https://doi.org/10.5281/zenodo.14517680 (2025).

Acknowledgements

This study was supported by the Key Project of the National Natural Science Foundation of China (grant number 52130804 to F.W.), National Social Science Fund of China (grant number 24VWB008 to F.W.), National Key Research and Development Program of China (grant number 2024YFC3808500 to F.W.) and National Natural Science Foundation of China Youth Program (grant number 52308042 to Y.D.). We thank X. Peng from Chinese Academy of Social Sciences, Z. Sun and Q. Zou from Wuhan University and H. Deng from Peking University for their guidance and support during the field research phase and data processing.

Author contributions

J.Z. conceptualized the research, curated the data, performed data analysis and contributed to investigation, methodology and the initial draft. F.W. developed the study's core idea, provided supervision and managed funding acquisition and project administration. Y.D. conducted data curation and data analysis and contributed to the initial draft. S.M. assisted with methodology, data curation and data analysis. C.Z. contributed to conceptualization, supervision and review. X.H. provided supervision and assisted with methodology and visualization. C.N., J.C. and Jianbao Liu contributed to conceptualization, supervision and review. Y.C. contributed to data curation and investigation. Jianguo Liu provided supervision and resources and supported conceptualization. Q.F. supported conceptualization, resources and supervision, and all authors contributed to the discussion of results and the final paper.

Competing interests

The authors declare no competing interests.

Additional information

Extended data is available for this paper at https://doi.org/10.1038/s44284-026-00446-8.

Supplementary information The online version contains supplementary material available at https://doi.org/10.1038/s44284-026-00446-8.

Correspondence and requests for materials should be addressed to Fang Wang.

Peer review information *Nature Cities* thanks W. Carleton, Vernon Scarborough and Gideon Shelach-Lavi for their contribution to the peer review of this work.

https://doi.org/10.1038/s44284-026-00446-8

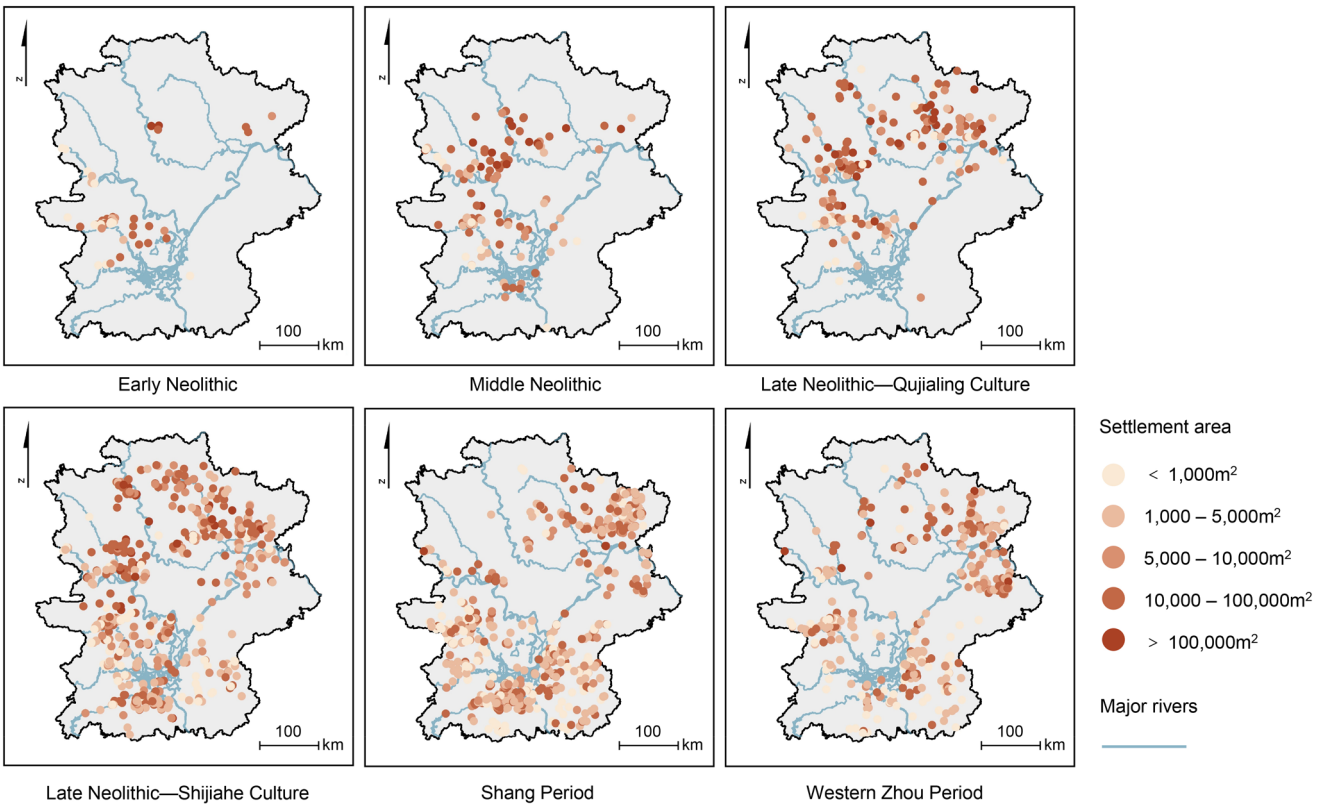

Extended Data Fig. 1 | Distribution of early settlements of varying sizes in the middle reaches of the Yangtze River Basin across six periods. Administrative boundaries from the Ministry of Natural Resources of the People's Republic of China (http://bzdt.ch.mnr.gov.cn/).

https://doi.org/10.1038/s44284-026-00446-8

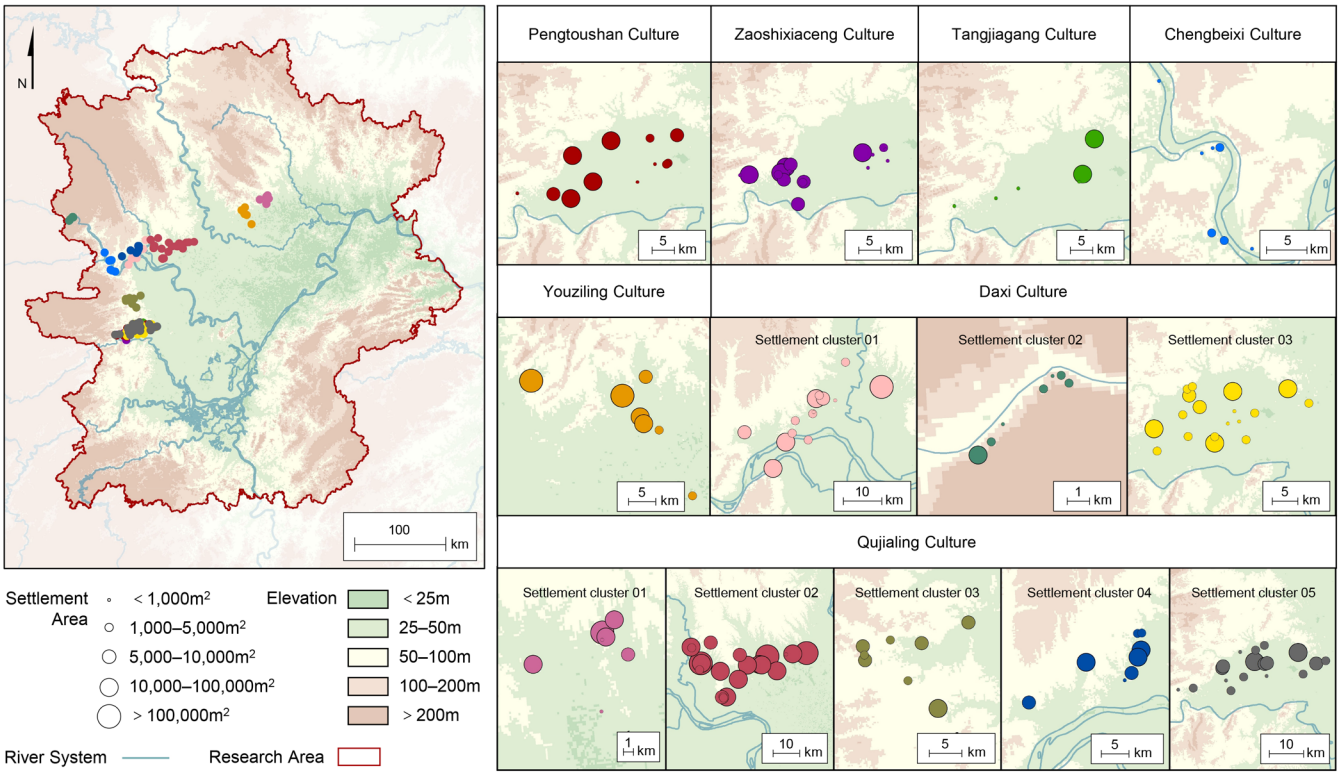

Extended Data Fig. 2 | Distribution map of early and middle Neolithic and Qujialing culture settlement clusters in the middle reaches of the Yangtze River Basin. Time ranges for each cultural period: Early Neolithic (8.5–6.3 ka BP): Pengtoushan (8.5–7.8 ka BP), Zaoshixiaceng (7.8–6.9 ka BP), Tangjiagang (6.9–6.3 ka BP), and Chengbeixi (7.8–6.3 ka BP) cultures; Middle Neolithic (6.3–5.3 ka BP): Daxi (6.3–5.5 ka BP) and Youziling (5.9–5.3 ka BP) cultures; Late Neolithic–Qujialing culture (5.3–4.5 ka BP): Qujialing culture. Administrative boundaries from the Ministry of Natural Resources of the People's Republic of China (http://bzdt.ch.mnr.gov.cn/).

https://doi.org/10.1038/s44284-026-00446-8

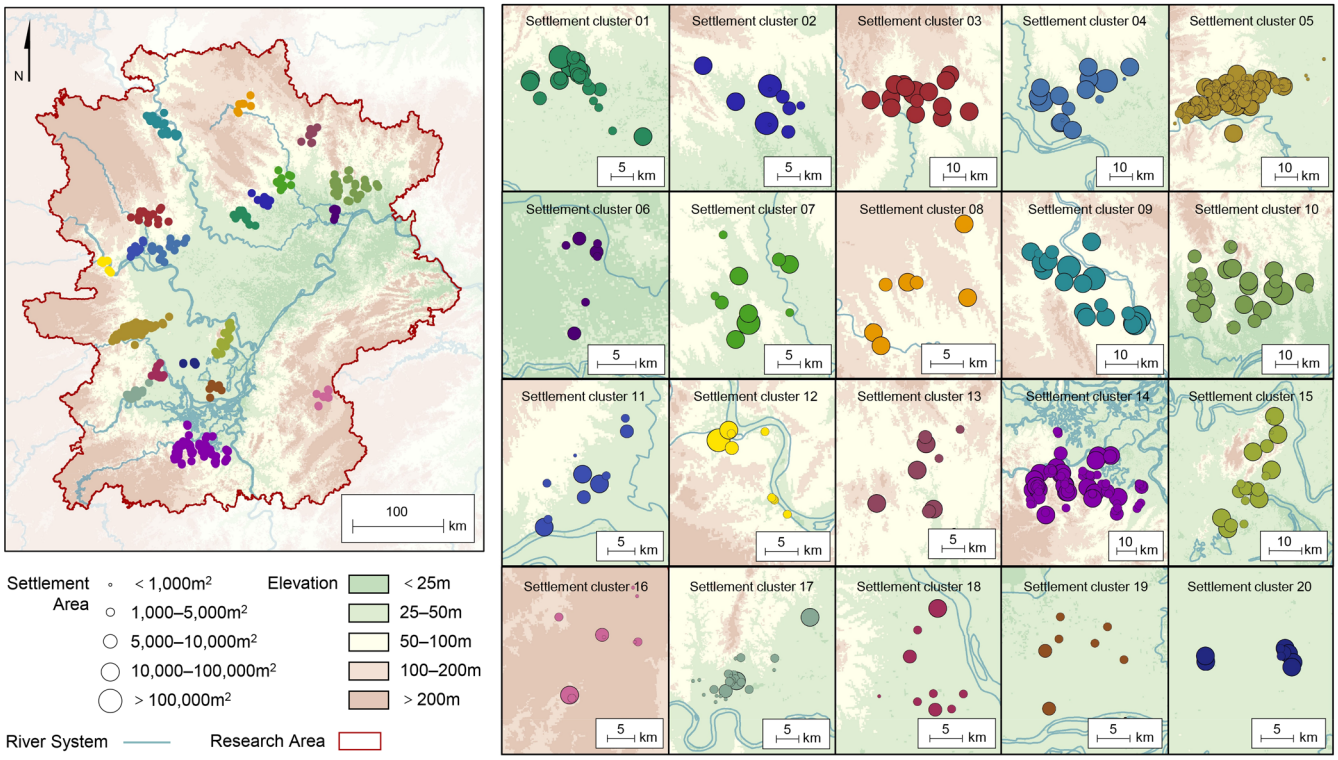

Extended Data Fig. 3 | Distribution map of Late Neolithic–Shijiahe culture (4.5–3.9 ka BP) settlement clusters in the middle reaches of the Yangtze River Basin. Administrative boundaries from the Ministry of Natural Resources of the People's Republic of China (http://bzdt.ch.mnr.gov.cn/).

https://doi.org/10.1038/s44284-026-00446-8

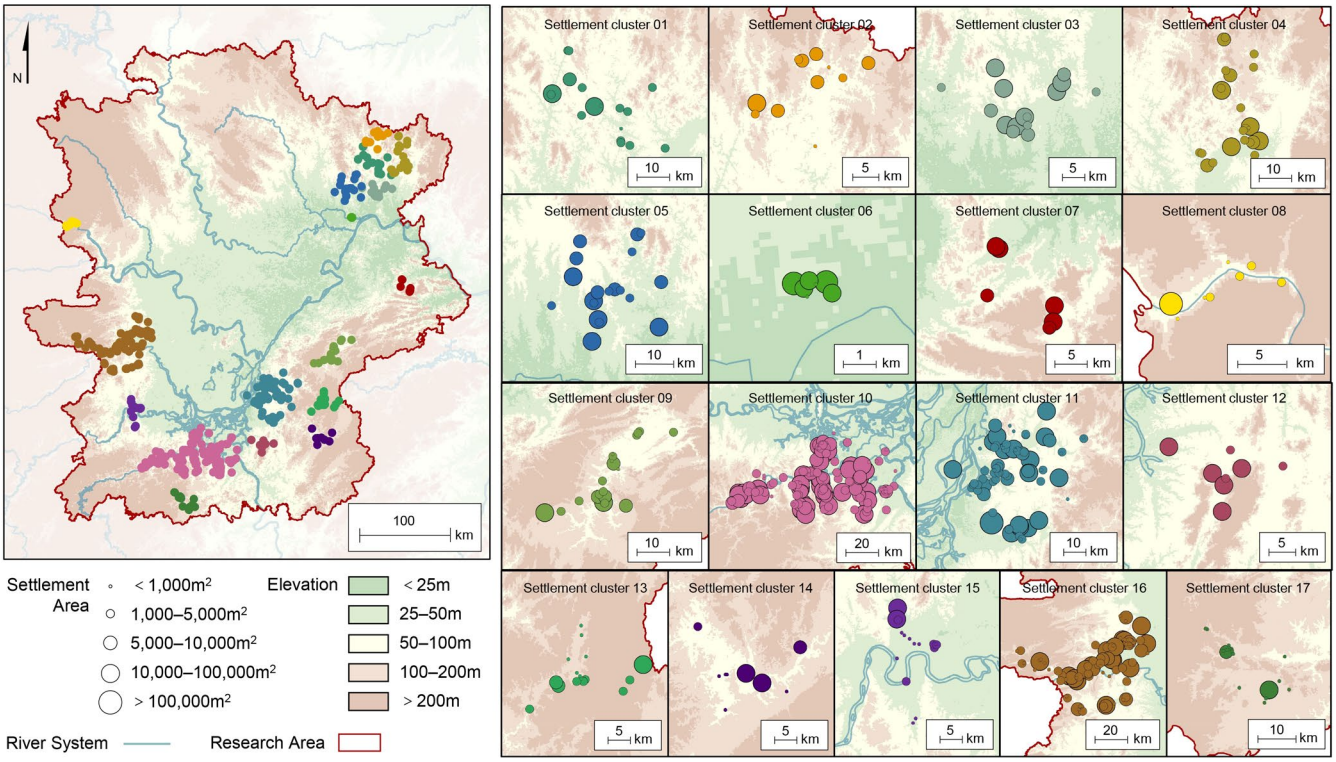

Extended Data Fig. 4 | Distribution map of Shang period (3.55–2.996 ka BP) settlement clusters in the middle reaches of the Yangtze River Basin. Administrative boundaries from the Ministry of Natural Resources of the People's Republic of China (http://bzdt.ch.mnr.gov.cn/).

https://doi.org/10.1038/s44284-026-00446-8

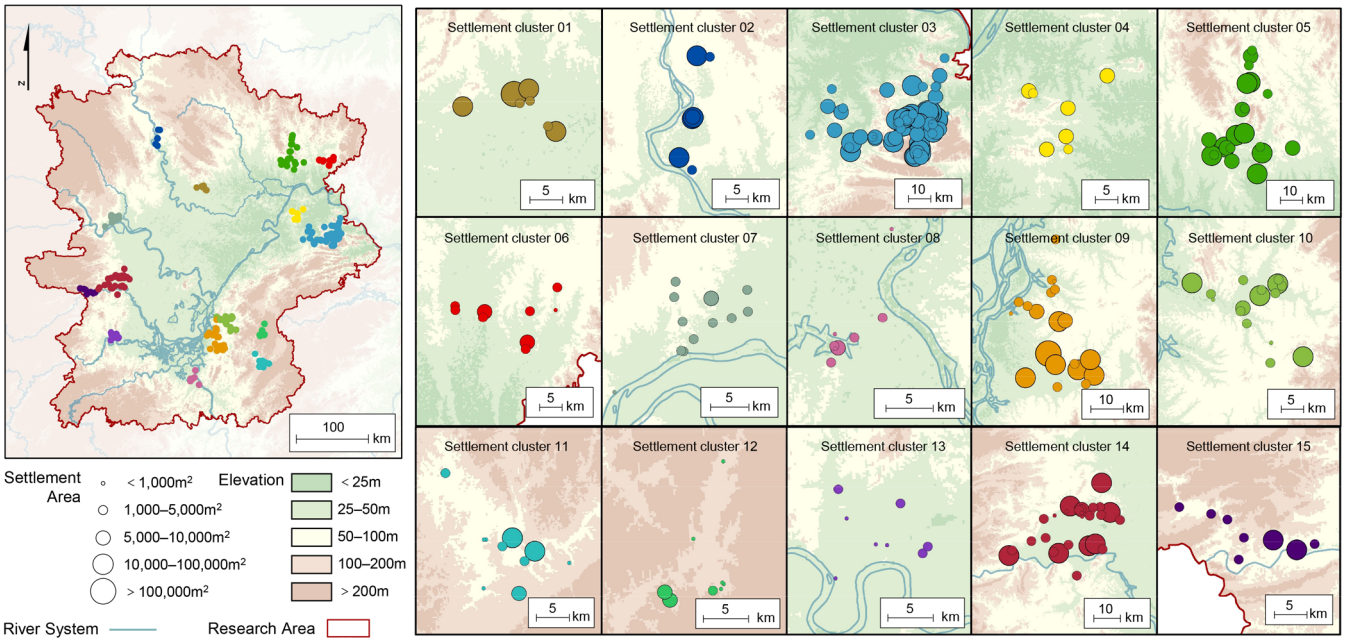

Extended Data Fig. 5 | Distribution map of Western Zhou period (2.996–2.72 ka BP) settlement clusters in the middle reaches of the Yangtze River Basin. Administrative boundaries from the Ministry of Natural Resources of the People's Republic of China (http://bzdt.ch.mnr.gov.cn/).

https://doi.org/10.1038/s44284-026-00446-8

Extended Data Table 1 | Settlement size distribution in the middle reaches of the Yangtze River Basin across different periods

Period	Area (m^2)									
	Small Settlements ≤1,000		Medium-Small Settlements 1,000~5,000		Medium Settlements 5,000~10,000		Large Settlements 10,000~100,000		Extra-Large Settlements > 100,000	
	Quantity	Proportion	Quantity	Proportion	Quantity	Proportion	Quantity	Proportion	Quantity	Proportion
Early Neolithic	6	11.5%	12	23.1%	5	9.6%	27	51.9%	2	3.9%
Middle Neolithic	10	8.1%	34	27.4%	17	13.7%	50	40.3%	13	10.5%
Late Neolithic—Qujialing Culture	11	5.9%	36	19.5%	27	14.6%	83	44.9%	28	15.1%
Late Neolithic—Shijiahe Culture	62	9.3%	195	29.1%	144	21.5%	240	35.9%	28	4.2%
Shang Dynasty	82	12.6%	244	37.7%	140	21.6%	173	26.7%	9	1.4%
Western Zhou Dynasty	34	9.1%	132	35.1%	84	22.3%	112	29.8%	14	3.7%

https://doi.org/10.1038/s44284-026-00446-8

Extended Data Table 2 | Distribution of settlement distances to the nearest river class in the middle reaches of the Yangtze River Basin across different periods

Period	Distance to the nearest river grade											
	First-class River		Second-class River		Third-class River		Fourth-class River		Fifth-class River		Sixth-class River	
	Quantity	Proportion	Quantity	Proportion	Quantity	Proportion	Quantity	Proportion	Quantity	Proportion	Quantity	Proportion
Early Neolithic	6	9.8%	0	0	12	19.7%	3	4.9%	11	18.0%	29	47.6%
Middle Neolithic	9	7.2%	3	2.4%	17	13.6%	9	7.2%	26	20.8%	61	48.8%
Late Neolithic—Qujialing Culture	5	2.6%	4	2.1%	11	5.7%	17	8.8%	42	21.9%	113	58.9%
Late Neolithic—Shijiahe Culture	10	1.5%	12	1.8%	83	12.2%	53	7.8%	166	24.5%	354	52.2%
Shang Dynasty	11	1.6%	8	1.2%	75	11.0%	81	11.8%	138	20.2%	371	54.2%
Western Zhou Dynasty	7	1.8%	7	1.8%	20	5.0%	54	13.7%	80	20.2%	227	57.5%

https://doi.org/10.1038/s44284-026-00446-8

Extended Data Table 3 | Percent contribution and permutation importance of the environmental variables included in the maximum entropy model across different periods

Period	Variable	Percent Contribution	Permutation Importance	Period	Variable	Percent Contribution	Permutation Importance
Early Neolithic	VD	32.9	25.5	Middle Neolithic	VD	41.8	39
	DMS	25.8	35.4		DMS	30.3	17.9
	PRCP	23.2	6.5		S	5.6	3.6
	S	4.7	5.2		DR	5.1	5.8
	DR	4.5	4.1		TEMP	4.6	11.9
	WEI	3.2	5.5		WEI	4	5.5
	TWI	2.1	3.6		A	2.9	2
	TO	1.6	10.9		TWI	2.7	5.9
	A	1.3	0.6		PRCP	2.4	1
	DRI	0.6	2.3		PLC	0.3	4.5
	PLC	0.1	0.3		PRC	0.2	2.7
					TPI	0.1	0.3
Late Neolithic—Qujialing Culture	DMS	69.9	55.1	Late Neolithic—Shijiahe Culture	DMS	28	8.6
	LSF	6.2	4.8		WEI	22.2	38.4
	VD	5.7	5.5		S	19.1	1.5
	WEI	4	9.6		TEMP	8.6	3.4
	A	3	3		PRCP	5.4	9.9
	DR	2.8	3.7		DR	4.1	4.5
	PRCP	2.8	3.5		TWI	3.7	4.9
	TWI	2.5	3.8		TO	2.6	12.9
	S	2.1	4.3		PLC	2.3	9.6
	DRI	0.5	0.4		VD	2.2	0.6
	PLC	0.3	6.4		A	0.9	1
					TPI	0.7	4.2
					DRI	0.3	0.6
Shang period	WEI	44.5	33.4	Western Zhou period	DMS	37.1	11.7
	TEMP	16.2	26.7		WEI	24.9	34.5
	LSF	9.8	2.2		TEMP	9.1	12.2
	DR	7	3.4		LSF	7.1	3.7
	TO	3.2	1.1		DR	6.1	2.9
	PLC	3.1	4.2		S	2.9	2.8
	DMS	2.9	2.7		VD	2.5	5.6
	TPI	2.8	4.5		TO	2.4	2.8
	VD	2.4	9.7		TWI	2.2	4.3
	TWI	2	1.7		PLC	2.1	7
	PRCP	1.9	5		A	1.4	1.3
	A	1.2	0.4		PRCP	1.1	5.1
	S	1.2	1.2		TPI	0.8	5.3
	PRC	1.1	2.2		DRI	0.3	0.8
	DRI	0.6	1.7				

nature portfolio

Corresponding author(s): Fang Wang

Last updated by author(s): Apr 15, 2026

Reporting Summary

Nature Portfolio wishes to improve the reproducibility of the work that we publish. This form provides structure for consistency and transparency in reporting. For further information on Nature Portfolio policies, see our Editorial Policies and the Editorial Policy Checklist.

Statistics

For all statistical analyses, confirm that the following items are present in the figure legend, table legend, main text, or Methods section.

n/a	Confirmed	
☐	☒	The exact sample size (*n*) for each experimental group/condition, given as a discrete number and unit of measurement
☐	☒	A statement on whether measurements were taken from distinct samples or whether the same sample was measured repeatedly
☒	☐	The statistical test(s) used AND whether they are one- or two-sided *Only common tests should be described solely by name; describe more complex techniques in the Methods section.*
☐	☒	A description of all covariates tested
☐	☒	A description of any assumptions or corrections, such as tests of normality and adjustment for multiple comparisons
☐	☒	A full description of the statistical parameters including central tendency (e.g. means) or other basic estimates (e.g. regression coefficient) AND variation (e.g. standard deviation) or associated estimates of uncertainty (e.g. confidence intervals)
☒	☐	For null hypothesis testing, the test statistic (e.g. *F*, *t*, *r*) with confidence intervals, effect sizes, degrees of freedom and *P* value noted *Give P values as exact values whenever suitable.*
☒	☐	For Bayesian analysis, information on the choice of priors and Markov chain Monte Carlo settings
☒	☐	For hierarchical and complex designs, identification of the appropriate level for tests and full reporting of outcomes
☒	☐	Estimates of effect sizes (e.g. Cohen's *d*, Pearson's *r*), indicating how they were calculated

Our web collection on statistics for biologists contains articles on many of the points above.

Software and code

Policy information about availability of computer code

Data collection	Settlement points were vectorized and a corresponding spatial database was established using ArcGIS Pro 3.3.
Data analysis	No custom code was used in this study. Settlement clustering was conducted using the DBSCAN module in ArcGIS Pro 3.3. The Euclidean distances from each settlement to the nearest mega settlement and river were calculated using the Euclidean Distance tool in ArcGIS Pro 3.3. Some environmental variables were extracted from DEM data using the automated geoscience analysis system in SAGA GIS 7.9.0. Correlation analysis and statistical visualization were performed using OriginLab 2022. To analyze the mechanisms underlying the spatial patterns of water adaptation in settlements, the Maximum Entropy Model (MaxEnt) was employed and implemented using Maxent 3.4.4 software.

For manuscripts utilizing custom algorithms or software that are central to the research but not yet described in published literature, software must be made available to editors and reviewers. We strongly encourage code deposition in a community repository (e.g. GitHub). See the Nature Portfolio guidelines for submitting code & software for further information.

Data

Policy information about availability of data

All manuscripts must include a data availability statement. This statement should provide the following information, where applicable:

- Accession codes, unique identifiers, or web links for publicly available datasets
- A description of any restrictions on data availability
- For clinical datasets or third party data, please ensure that the statement adheres to our policy

The datasets used in this study, including the multi-period settlement point distributions in the Jianghan-Dongting Basin, as well as all input files for the MaxEnt model (settlement points by period, environmental variable layers, and the bias file), are available in the Zenodo repository: https://doi.org/10.5281/zenodo.14517680. Some data used in this study are from publicly available sources: the SRTM V4.1 DEMs can be accessed via the data search page at https://srtm.csi.cgiar.org/srtmdata/; the mid-Holocene CAS-FGOALS dataset is accessible at https://esgf-node.llnl.gov/search/cmip6/.

Research involving human participants, their data, or biological material

Policy information about studies with human participants or human data. See also policy information about sex, gender (identity/presentation), and sexual orientation and race, ethnicity and racism.

Reporting on sex and gender	N/A
Reporting on race, ethnicity, or other socially relevant groupings	N/A
Population characteristics	N/A
Recruitment	N/A
Ethics oversight	N/A

Note that full information on the approval of the study protocol must also be provided in the manuscript.

Field-specific reporting

Please select the one below that is the best fit for your research. If you are not sure, read the appropriate sections before making your selection.

☐ Life sciences ☐ Behavioural & social sciences ☒ Ecological, evolutionary & environmental sciences

For a reference copy of the document with all sections, see nature.com/documents/nr-reporting-summary-flat.pdf

Ecological, evolutionary & environmental sciences study design

All studies must disclose on these points even when the disclosure is negative.

Study description	We examine 2,106 early settlements dating from 8.5 to 2.72 ka BP in the middle reaches of the Yangtze River basin, focusing on the intertwined temporal trajectories of spatial pattern and hydrological adaptation. Using archaeological data and maximum entropy model, we trace how settlement distribution and hydrological conditions changed over time.
Research sample	The research sample consists of 2,106 archaeologically verified settlement locations dating from 8.5 to 2.7 ka BP, compiled from published sources and archaeological databases.
Sampling strategy	To account for potential sampling bias in archaeological survey data, we constructed a bias layer based on a kernel density estimation (KDE) of all known settlement locations across periods. The KDE was performed in ArcGIS Pro 3.3 using the Kernel Density tool. All 2,106 settlement points were used as input features. The output cell size was set to 250 meters to match the resolution of the environmental layers. The search radius was set to 100,000 meters, based on the exploratory sensitivity tests for optimal smoothing. The resulting raster bias layer highlights zones with higher densities of known settlements and serves as a proxy for differential survey effort, and was provided to MaxEnt to guide background point sampling. By weighting background points according to this bias file, we mitigate the influence of uneven survey effort on model estimation.
Data collection	All data used were secondary sources derived from archaeological publications, digital elevation models (DEM), and other open-access environmental datasets.
Timing and spatial scale	Settlement data span from 8.5 to 2.7 ka BP. The spatial analysis covers the middle Yangtze River region.
Data exclusions	No data were excluded from analysis. All settlements with complete spatial and temporal information were included.

Reproducibility	All procedures used in data processing and modeling are described in the Methods section.
Randomization	A random partitioning strategy was used within the Maxent modeling framework, in which 75% of the total settlement points were randomly selected as training data and 25% as testing data. This random split was repeated 10 times to ensure the robustness of the model and minimize sampling bias.
Blinding	N/A

Did the study involve field work? ☐ Yes ☒ No

Reporting for specific materials, systems and methods

We require information from authors about some types of materials, experimental systems and methods used in many studies. Here, indicate whether each material, system or method listed is relevant to your study. If you are not sure if a list item applies to your research, read the appropriate section before selecting a response.

Materials & experimental systems

n/a	Involved in the study
☒	☐ Antibodies
☒	☐ Eukaryotic cell lines
☐	☒ Palaeontology and archaeology
☒	☐ Animals and other organisms
☒	☐ Clinical data
☒	☐ Dual use research of concern
☒	☐ Plants

Methods

n/a	Involved in the study
☒	☐ ChIP-seq
☒	☐ Flow cytometry
☒	☐ MRI-based neuroimaging

Palaeontology and Archaeology

Specimen provenance	The study vectorized the settlement site information recorded in The Atlas of Chinese Cultural Relics: Hubei Volume and The Atlas of Chinese Cultural Relics: Hunan Volume, supplementing it with recent archaeological excavation reports from the relevant regions.
Specimen deposition	N/A
Dating methods	N/A

☐ Tick this box to confirm that the raw and calibrated dates are available in the paper or in Supplementary Information.

Ethics oversight	N/A

Note that full information on the approval of the study protocol must also be provided in the manuscript.

Plants

Seed stocks	N/A
Novel plant genotypes	N/A
Authentication	N/A